*Sensors and Materials*, Vol. 36, No. 6 (2024) 2509–2520
MYU Tokyo



S & M 3683

# Design of Microstrip Filtering Antenna for Point-to-point Communication of Automated Guided Vehicles

Tianwen Guo,[1] Yanggao Xu,[1] Yong Xie,[2] Xiaogang Li,[1*]
Dahui Lu,[1] Haitao Xing,[2] and Zhonghua Ma[2**]

[1]Longyan Tobacco Industry Co., Ltd., Longyan, Fujian 364000, China
[2]School of Marine Information Engineering, Jimei University, Xiamen, Fujian 361021, China

(Received January 15, 2024; accepted April 30, 2024)

***Keywords:*** filtering antenna, gain, microstrip resonator, low profile, U-shaped slot

A highly selective planar microstrip filtering antenna for point-to-point communication is proposed in this paper. The bandpass filter is composed of a rectangular split-ring coupling resonator, and a portion of the filter is equivalent to a microstrip monopole antenna. Two rectangular split-ring structures with their openings aligned generate resonant characteristics, and U-shaped microstrip coupling structures are wrapped outside to optimize the passband characteristics. One of the U-shaped microstrip structures is transformed into a one-side bent structure as a radiation unit and serves as the resonant structure of the final stage of the filter, reducing the connection loss between the filter and the antenna. The operating frequency band of the filtering antenna is from 6.38 to 6.63 GHz with a reflection coefficient of less than −10 dB, a fractional bandwidth of 3.8%, and a peak gain of 4.46 dBi. The filtering antenna has excellent frequency selectivity, good out-of-band suppression, high gain, and small device size, in addition to its low cost after system integration. The simulation results are consistent with the experimental test results. The filtering antenna as a novel radio frequency sensor can be applied to the point-to-point communication of automated guided vehicles in the logistics field.

## 1. Introduction

With the development of communication technology, higher requirements for the volume and performance of mobile terminals have been put forward by users. Antennas and filters are two very important functional modules in the RF front end. High-quality factor filters have strict requirements for components. Low insertion loss can improve the signal-to-noise ratio. Therefore, antennas and filters directly affect the quality of received and transmitted signals. The antenna mainly plays the role of transmitting and receiving signals. The filter selects the receiving signals of the antenna and suppresses the out-of-band signals. The filtering antenna has advantages of minor losses, low cost, and miniaturization, and has become an inevitable choice for terminals. The filtering antenna requires no microstrip conversion or coaxial cables to

*Corresponding author: e-mail: lxg22089@fjtic.cn
**Corresponding author: e-mail: mzhxm@jmu.edu.cn
https://doi.org/10.18494/SAM4857

connect the antenna and filter, resulting in minimal losses.[1,2] Therefore, the filtering antenna, which is a combination of an antenna and a filter has been widely studied.

The filtering antenna was first proposed by Schell and Mailloux.[3] The antenna integrates the function of the filter, achieving the filtering of transmitted and received signals, suppressing interference, and enhancing the performance and reliability of the communication system. In traditional communication systems, antennas and filters are designed separately, and their correlation is low. Therefore, an additional matching circuit is required to connect the antenna and the filter, which increases the complexity of the design and occupies a large space. Moreover, filters can cause significant insertion losses. For the above shortcomings, the integrated design of antennas and filters has become the direction of future communication system design.

The design methods for filtering antennas mainly include the direct cascading method,[4–6] equivalent substitution method,[7,8] and fusion design method.[9–13] Direct cascading is the process of connecting the input port of the antenna and the output port of the filter according to the same characteristic impedance, achieving direct impedance matching with minimal energy loss. However, direct cascading requires an additional impedance-matching circuit, leading to increased size and insertion loss. In the equivalent substitution method, the last-order resonator of the filter is replaced by a radiating antenna, which reduces the size of the entire device and cuts down the transmission loss between the filter and the antenna. On the basis of the antenna structure, the fusion design method realizes the filtering function by stacking patches,[9] adding parasitic components,[10,11] and adding slots.[12,13] This method can realize the miniaturization and high gain of filtering antennas, but the radiation performance will deteriorate.

The design of filtering antennas is much more complex than that of traditional antennas, and the direct cascading method results in a larger dimension and a higher insertion loss. Although the fusion design method reduces the size of the antenna, it can distort the radiation pattern of the antenna. The equivalent substitution method can be used in filtering the design of the antenna to reduce its size, decrease the insertion loss, and optimize the radiation pattern. Yan *et al.* proposed a filtering antenna for a wireless local area network communication system, which consists of four U-shaped microstrip resonators, one Γ-shaped antenna, and one parallel coupling line.[7] The maximum gain of this filtering antenna is 3.059 dBi in the operating frequency band. The out-of-band gain is reduced to below −24 dBi. Chuang and Chung proposed a filter structure composed of microstrip lines and a coplanar waveguide, in which broadside coupling is adopted into the Γ-shaped antenna area.[8] This filtering antenna provides a high band-edge selectivity but a low-passband-gain response. On the basis of the Butterworth bandpass filter, Chen *et al.* used a sector patch antenna with a defected ground structure (DGS) to replace the resonator at the output end of the filter, forming a filtering antenna.[14] The passband bandwidth of the filtering antenna is 460 MHz, with a peak gain of 2.3 dBi in the passband, and the passband edge has good frequency selectivity. As described in Ref. 15, two pairs of stepped impedance resonators (SIRs) and a square patch were used to form a filtering antenna, where the SIR resonates with the edges of the square patch, obtaining good filtering characteristics.

Many scholars have also proposed filtering antennas based on the substrate integrated waveguide (SIW),[16–18] which have high-quality factors, good bandpass characteristics, and out-of-band attenuation characteristics. However, the design of these antennas is based on multilayer printed circuit board structures, which are complex and have high costs.

In this paper, a low-profile and high-selectivity filtering antenna is proposed. This filtering antenna consists of two rectangular split-ring resonators, a U-shaped microstrip coupling structure, and a deformed radiation microstrip unit with a U-shaped microstrip coupling structure. The two rectangular split-ring resonators achieve a bandpass response, and the U-shaped microstrip coupling structure attains tight coupling, which further promotes filtering responses. This method of the equivalent substitution of filter elements makes the transmission loss close to zero. Compared with the direct cascading method, it avoids the transition from lossy slots to microstrip[19] and bulky coaxial connectors.[20] The antenna proposed in this paper adopts a simple microstrip planar structure, which is easy to manufacture and adjust. As a novel RF sensor, it is suitable for the 5G and point-to-point communication of automated guided vehicles in specific scenarios.

## 2. Design and Analysis of Filtering Antenna

The filtering antenna is designed on a Rogers 4350B substrate, with a dielectric constant of 3.66, a loss tangent of 0.004, and a thickness of 0.762 mm. The antenna is simulated and designed with a high-frequency simulator structure (HFSS).

### 2.1 Filter design

The bandpass filter consists of resonant coupling structures at the dielectric substrate top layer and the ground plate at the dielectric substrate bottom layer. The structure of the bandpass filter is shown in Fig. 1. Two half-wavelength rectangular split-ring resonators are wrapped with two U-shaped microstrip coupling structures, with the openings of the rectangular split-rings aligned with a spacing of $s_2$. The input and output ports of the filter are connected to the two U-shaped microstrips through the 50-ohm-characteristic-impedance microstrip line. Two rectangular split-ring resonators form the resonant structure. The length and width of the rectangular split-ring resonator are $y_6$ and $x_1$, respectively. The microstrip width of the rectangular split-ring is $w_1$, the coupling spacing is $s_2$, and the opening length is $C$. The side

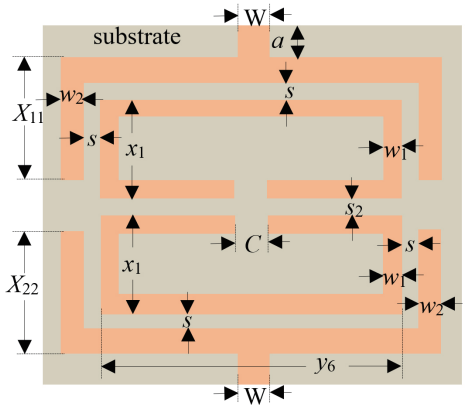


Fig. 1. (Color online) Structure of bandpass filter.

lengths of the two U-shaped coupling microstrips are $X_{11}$ and $X_{22}$. The U-shaped microstrip width is $w_2$ and the spacing between the rectangular split-ring resonator and the U-shaped coupled microstrip is $s$.

The substrate dimensions of the filter are 16.7 × 20.2 mm$^2$. After optimization with HFSS, the final structural parameters of this bandpass filter are as shown in Table 1. Figure 2 shows the resonance curve of the bandpass filter simulated under the structural parameters shown in Table 1. The frequency band with a return loss of less than −10 dB is from 6.37 to 6.65 GHz, as shown in Fig. 2. The bandwidth of the filter is 280 MHz and the fractional bandwidth is 4.3%. The insertion loss is 0.9 dB at a center frequency of 6.5 GHz. The out-of-band suppression of the transmission characteristics reached −20 dB at 5.67 and 7.03 GHz, demonstrating good stopband suppression characteristics.

## 2.2 Antenna design

The antenna unit is a U-shaped microstrip with one side bent, and the filter is a microstrip coupling structure. Figure 3 is a schematic of the structure of the microstrip monopole antenna. The directions of the $x$- and $y$-axes in the rectangular coordinate system are shown in Fig. 3, and the direction of the $z$-axis is perpendicular to the $xoy$-plane. One side of the U-shaped microstrip monopole antenna is bent. The resonance frequency of the antenna is determined by the length $l_{11} + l_{22} + l_{33}$ of the U-shaped microstrip. There is a grounding plate on the back surface of the antenna substrate that is slightly shorter than the feeder line to improve the input impedance of the antenna. Table 2 shows the specific structural parameter values of the microstrip monopole antenna.

Table 1
Structure parameters of the bandpass filter (unit: mm).

| $W$ | $w_1$ | $w_2$ | $s$ | $s_1$ | $s_2$ | $x_1$ | $C$ | $X_{11}$ | $X_{22}$ | $y_6$ | $h$ |
|---|---|---|---|---|---|---|---|---|---|---|---|
| 1.8 | 0.7 | 0.8 | 0.2 | 0.4 | 0.5 | 5 | 1.5 | 5.9 | 6.1 | 12.2 | 0.762 |

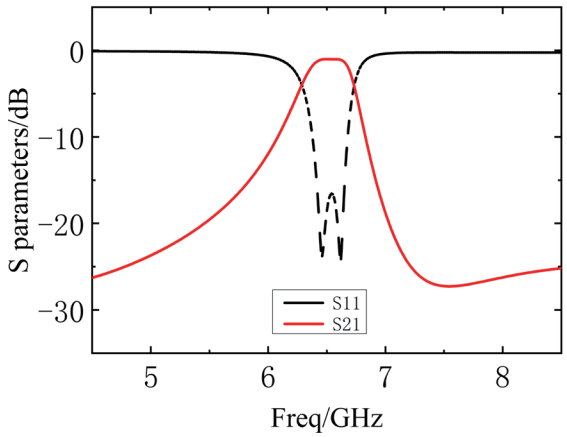


Fig. 2. (Color online) Resonant curve of the bandpass filter when $X_{11}$ = 5.9 mm and $X_{22}$ = 6.1 mm.

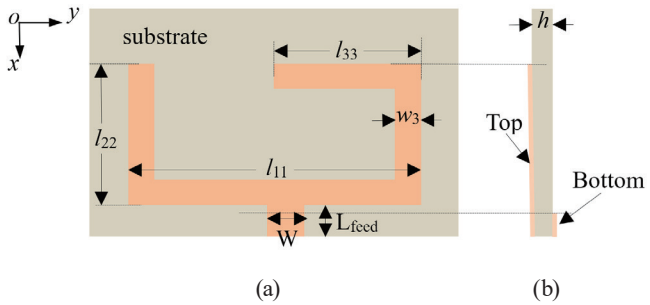


Fig. 3. (Color online) Structure of the microstrip monopole antenna. (a) Top and (b) side views.

Table 2
Structure parameters of antenna (unit: mm).

| $W$ | $l_{11}$ | $l_{22}$ | $l_{33}$ | $L_{feed}$ | $w_3$ | $h$ |
|---|---|---|---|---|---|---|
| 1.8 | 18 | 10 | 8 | 2 | 1 | 0.762 |

The reflection coefficient simulation result of the microstrip monopole antenna is shown in Fig. 4. The reflection coefficient is −29.28 dB at a center frequency of 6.5 GHz. The frequency with a reflection coefficient of less than −10 dB ranges from 5.65 to 7.17 GHz. The impedance bandwidth reaches 1.52 GHz.

The current distribution of this monopole antenna is shown in Fig. 5, with the current flowing from the feeding point to the end on both arms. Figure 6 shows that the axial ratios (ARs) are much greater than 3 dB near 6.5 GHz, indicating that the antenna is linearly polarized.

Figure 7 shows the radiation patterns of the microstrip monopole antenna at the center frequency of 6.5 GHz. The pattern radiates in a butterfly shape on the *xoz*-plane and a quasi-elliptical shape on the *yoz*-plane. The simulation cross polarizations of the *xoz*- and *yoz*-planes are both below −20 dB.

## 3. Simulation of Filtering Antenna

After deforming the part of the U-shaped coupling microstrip structure in Fig. 1 into a microstrip monopole antenna in Fig. 3, the filtering antenna structure is as shown in Fig. 8. Figure 8(a) is a schematic of the top view of the filtering antenna, and the side view is shown in Fig. 8(b). The back of the filtering antenna radiation structure does not have a ground plate; only the back of the rectangular split-ring resonator has a ground plate.

The simulated reflection coefficient and realized gain of the proposed antenna are shown in Fig. 9. The high roll-off rate between the passband and stopband of the antenna in Fig. 9 is attributed to the tight coupling of the resonator. The frequency band is from 6.39 to 6.63 GHz with a reflection coefficient of less than −10 dB, the bandwidth of the antenna is 240 MHz, and the fractional bandwidth is 3.69%. The reflection coefficient is −25.9 dB at a central operating frequency of 6.5 GHz. Figure 10 shows the *xoz*-plane and *yoz*-plane radiation patterns of the filtering antenna at an operating frequency of 6.5 GHz. The simulated copolarization in the radiation direction in both *xoz*- and *yoz*-planes is at least 15 dB higher than the corresponding cross-polarization.

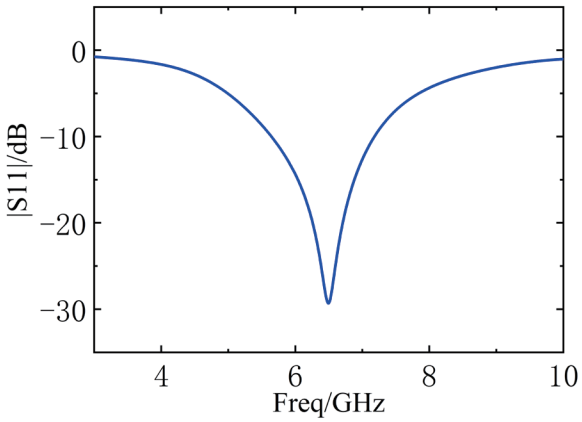


Fig. 4. (Color online) Simulated reflection coefficient of the microstrip monopole antenna.

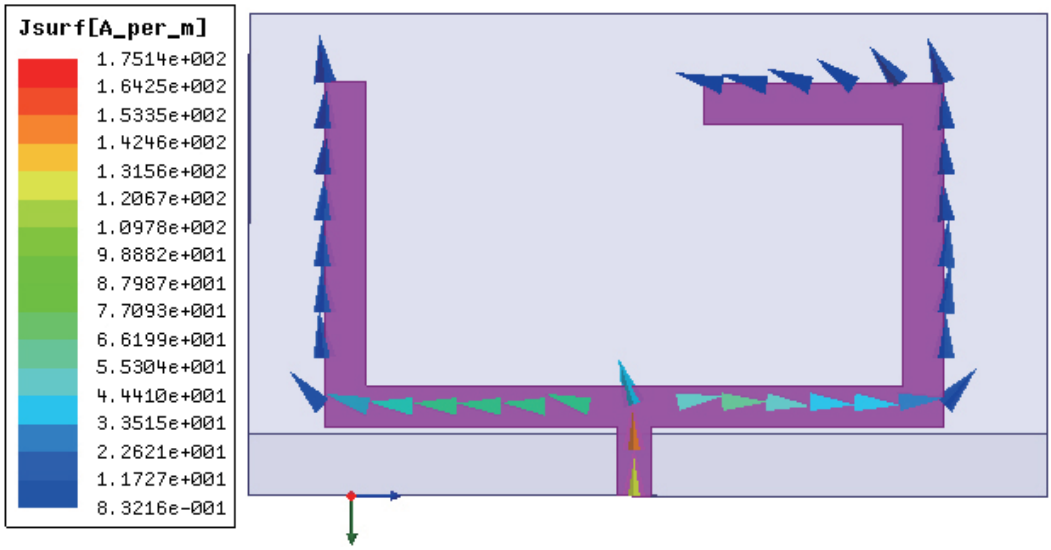


Fig. 5. (Color online) Current distribution of the monopole antenna.

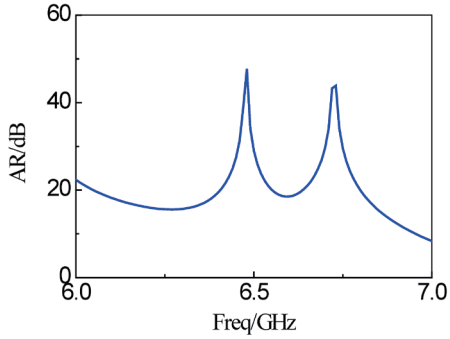


Fig. 6. (Color online) AR curve of the monopole antenna.

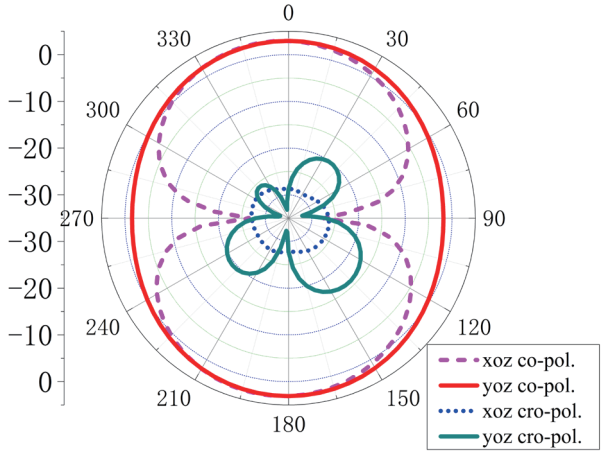


Fig. 7. (Color online) Radiation patterns of the proposed antenna at 6.5 GHz.

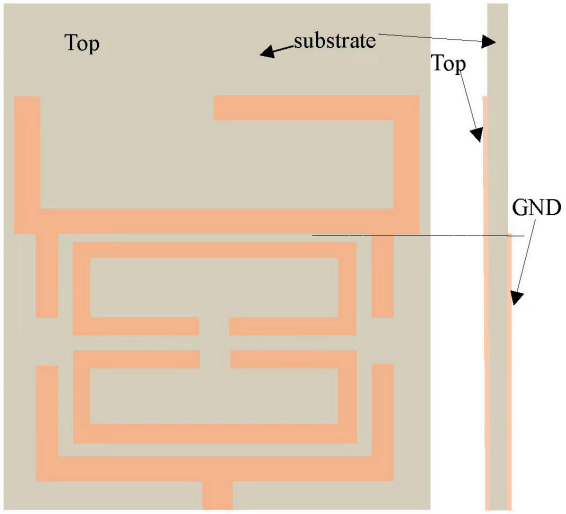


(a) (b)

Fig. 8. (Color online) Filtering antenna structure. (a) Top and (b) side views.

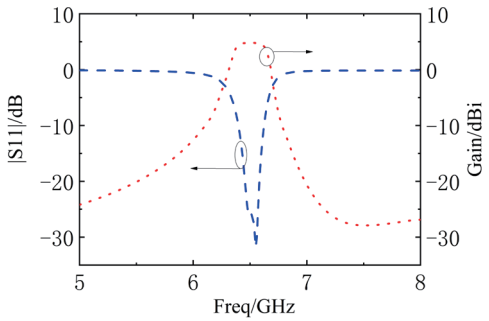


Fig. 9. (Color online) Simulated reflection coefficient and realized gain of the proposed antenna.

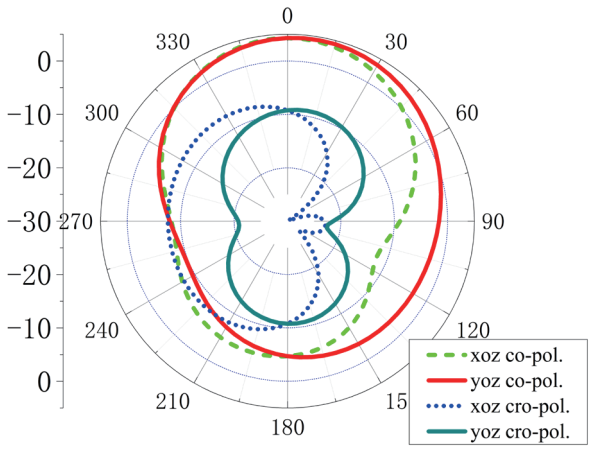


Fig. 10. (Color online) Simulated patterns of the filtering antenna in *xoz*- and *yoz*-planes at 6.5 GHz.

## 4. Measurement Results

To verify the proposed filtering antenna, the prototype of the filtering antenna fabricated on a Rogers 4350B substrate is shown in Fig. 11. The filtering antenna has small dimensions of $0.7\lambda_0 \times 0.49\lambda_0 \times 0.0185\lambda_0$. The simulated and measured gains of the filtering antenna are illustrated in Fig. 12. It can be seen that the gain is high and the reflection coefficient is low within the passband and the simulation results agree with the measurements results. The frequency range varies from 6.38 to 6.63 GHz with the measured reflection coefficient at less than −10 dB. The impedance bandwidth reaches 250 MHz. The measured reflection coefficient at a center frequency of 6.5 GHz is −24.16 dB. The measured peak gain fluctuates between 2.7 and 4.46 dBi within the passband. The measured and simulated values fluctuate within the range of 0.01 to 0.51 dB. The measured gain in the passband is slightly lower than the simulated result, whereas the measured reflection coefficient is slightly higher than the simulated result. There is a significant difference between the measured and simulated results of out-of-band gain suppression. After analyzing the measured results, it is speculated that the reason may be that the impedance mismatch of the antenna outside the passband during measurement caused losses.

Figure 13 shows the measured voltage standing wave ratio (*VSWR*) curve of the antenna. The *VSWR*s are 2 at a frequency of 6.39 GHz, 1.8 at a frequency of 6.62 GHz, and 1.11 at a center frequency of 6.5 GHz.

At a center frequency of 6.5 GHz, the measured radiation patterns of the *xoz*- and *yoz*-planes of the filtering antenna are as shown in Fig. 14. The main radiation direction of the antenna is in the 0° direction. There is a difference between the simulation and measurement results of the antenna pattern, mainly due to the shaking of the turntable in the anechoic chamber and the slight shaking of the test antenna during rotation. Moreover, SMA connectors were not taken into account during the simulation, and the solder joints on the feed line of the SMA connector also had a certain impact on the antenna pattern.

Table 3 provides a comprehensive comparison between the recently reported and proposed filtering antennas. Although the filtering antenna in Ref. 20 has good in-band reflection and

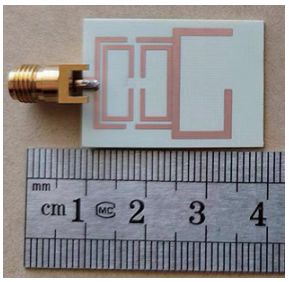


Fig. 11. (Color online) Photograph of the fabricated filtering antenna.

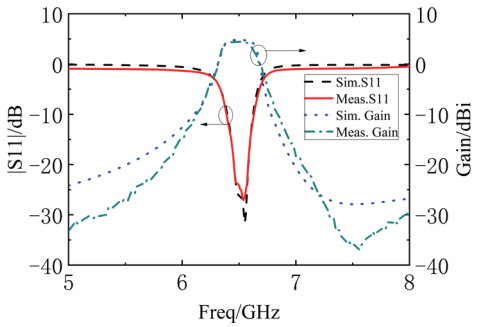


Fig. 12. (Color online) Simulated and measured reflection coefficients and realized gains of the filtering antenna.

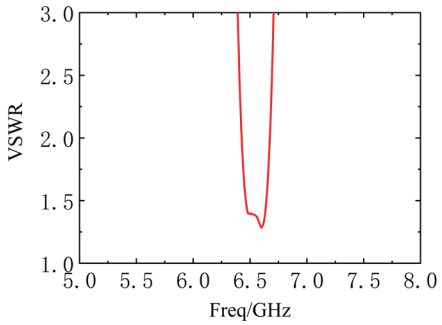


Fig. 13. (Color online) Measurement result of *VSWR* of the filtering antenna.

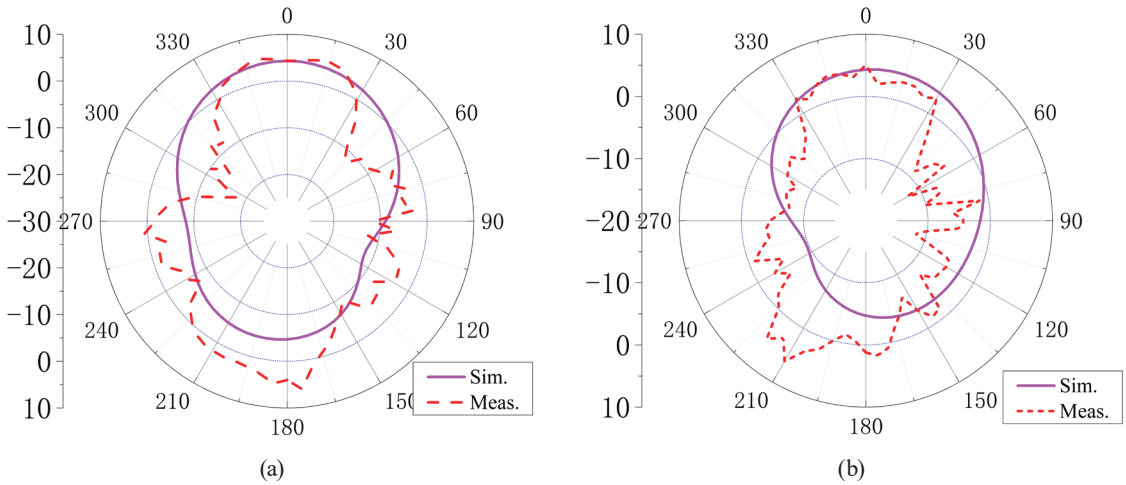


Fig. 14. (Color online) Measured radiation patterns of the filtering antenna at 6.5 GHz. (a) *xoz*- and (b) *yoz*-planes.

Table 3
Comparison between the performance characteristics of the previously reported filtering antennas and this work.

| Ref. | $f_0$ (GHz) | *FBW (%)* | Dimensions ($\lambda_0^3$mm$^3$) | Peak gain (dBi) | Rejection level (dB) |
|---|---|---|---|---|---|
| [20] | 5.16 | 2.5 | 1.08 × 1.02 × 0.009 | 6.79 | 28 |
| [21] | 5.5 | 2.6 | 0.8 × 0.48 × 0.014 | 4.3 | 22 |
| [22] | 2.44 | 4.1 | 0.89 × 0.89 × 0.154 | 5.1 | 14 |
| [23] | 2.84 | 9.2 | 0.63 × 0.47 × 0.015 | 5.75 | 11 |
| [24] | 2.77 | 5.1 | 0.75 × 0.45 × 0.015 | 6.3 | 14 |
| This work | 6.5 | 3.8 | 0.7 × 0.49 × 0.0185 | 4.46 | 24 |

high gain, the proposed filtering antenna has a smaller size and a wider impedance bandwidth of −10 dB. Compared with the filtering antennas in Refs. 21–24, the proposed filtering antenna has higher reflection characteristics within the passband. The size and gain of the antenna are also relatively appropriate. The impedance bandwidth of −10 dB is larger than those in Refs. 20–22.

## 5. Conclusions

In this study, a low-profile and high-selectivity microstrip filtering antenna was demonstrated. The filtering antenna includes two rectangular split-ring resonators and a U-shaped coupled microstrip; the U-shaped coupled microstrip was deformed into a microstrip monopole to form a radiation unit. Finally, the filtering antenna was manufactured and tested, and the results showed that the filtering antenna has excellent out-of-band suppression characteristics, good rectangular coefficient, and a small reflection within the passband. The filtering antenna has a simple structure, a low cost, and stable in-band radiation characteristics. The simulation and test results are good and consistent within the passband of the filtering antenna. The proposed filtering antenna has a low insert loss, small dimensions, and excellent performance. As RF sensors, it holds great potential in communications in IoT and logistics fields.

## Acknowledgments

This work was supported by China Tobacco Fujian Industry Co., Ltd. 2023 External Technical Cooperation Project (FJZYHZJH2023018).

## References

1 B. Liu, X. Gong, and W. J. Chappell: IEEE Trans. Microwave Theory Tech. **52** (2004) 2567. https://doi.org/10.1109/TMTT.2004.837165
2 K. Ahn and I. Yom: 2008 IEEE MTT-S Int. Microwave Symposium Digest (IEEE, 2008) 1235.
3 A. C. Schell and R. J. Mailloux: US19780904964 [P]. 1979 US4169268A.
4 C. X. Mao, S. Gao, Y. Wang, Q. Fan, and Q. X. Chu: IEEE Trans. Antennas Propag. **63** (2015) 5492. https://doi.org/10.1109/TAP.2015.2496099
5 Y. T. Liu, K. W. Leung, and N. Yang: IEEE Trans. Antennas Propag. **68** (2020) 633. https://doi.org/10.1109/TAP.2019.2938798
6 C. Y. Hsieh, C. H. Wu, and T. G. Ma: IEEE Antennas Wirel. Propag. Lett. **14** (2015) 1056. https://doi.org/10.1109/LAWP.2015.2390033

7 S. J. Yan, C. Q. Zhang, Q. Chen, and M. S. Tong: Appl. Comput. Electromagn. Soc. J. **37** (2022) 996. https://doi.org/10.13052/2022.ACES.J.370909
8 C. T. Chuang and S. J. Chung: IEEE Trans. Antennas Propag. **59** (2011) 3630. https://doi.org/10.1109/TAP.2011.2163777
9 M. Tian, N. N. Yan, Y. Luo, and K. X. Ma: IEEE Antennas Wirel. Propag. Lett. **20** (2021) 2270. https://doi.org/10.1109/LAWP.2021.3106908
10 C. F. Ding, Z. Y. Zhang, and Y. M. Zeng: IEEE Trans. Antennas Propag. **71** (2023) 1931. https://doi.org/10.1109/TAP.2022.3233649
11 M. Li, S. J. Tian, M. C. Tang, and L. Zhu: IEEE Trans. Antennas Propag. **70** (2022) 1511. https://doi.org/10.1109/TAP.2021.3111638
12 J. Y. Jin, S. W. Liao, and Q. Xue: IEEE Trans. Antennas Propag. **66** (2018) 2125. https://doi.org/10.1109/TAP.2018.2804661
13 X. C. Shao, L. W. Deng, C. X. Zhou, T. Yan, C. Tang, X. H. Gao, and L. L. Qiu: Arabian J. Sci. Eng. **48** (2023) 6831. https://doi.org/10.1007/s13369-022-07598-4
14 X. W. Chen, F. X. Zhao, L. Y. Yan, and W. M. Zhang: IEEE Antennas Wirel. Propag. Lett. **12** (2013) 857. https://doi.org/10.1109/LAWP.2013.2271972
15 H. Y. Huang, K. Z. Hu, J. Deng, D. Yan, J. F. Xie, and Y. Zhang: Microwave Opt. Technol. Lett. **65** (2023) 1982. https://doi.org/10.1002/mop.33638
16 Y. Yusuf, H. T. Cheng, and X. Gong: IEEE Trans. Antennas Propag. **59** (2011) 4016. https://doi.org/10.1109/TAP.2011.2164186
17 S. C. Tang, X. Y. Wang, W. Yu, W. W. Yang, and J. X. Chen: IEEE Antennas Wirel. Propag. Lett. **22** (2023) 268. https://doi.org/10.1109/LAWP.2022.3208861
18 S. S. Ji, Y. D. Dong, Y. S. Pan, Y. L. Zhu, and Y. Fan: IEEE Trans. Antennas Propag. **69** (2021) 3155. https://doi.org/10.1109/TAP.2020.3037819
19 T. M. Shen, C. F. Chen, T. Y. Huang, and R. B. Wu: IEEE Trans. Microwave Theory Tech. **55** (2007) 1771. https://doi.org/10.1109/TMTT.2007.902080
20 L. Li, D. Pang, Y. B. Feng, Q. Wang, and Z. Y. Lei: IEEE Antennas Wirel. Propag. Lett. **18** (2019) 2503. https://doi.org/10.1109/LAWP.2019.2941534
21 K. Dhwaj, J. M. Kovitz, H. Z. Tian, L. J. Jiang, and T. Itoh: IEEE Antennas Wirel. Propag. Lett. **17** (2018) 833. https://doi.org/10.1109/LAWP.2018.2818058
22 Y. T. Liu, K. W. Leung, J. Ren, and Y. X. Sun: IEEE Trans. Antennas Propag. **67** (2019) 3629. https://doi.org/10.1109/TAP.2019.2902670
23 K. Z. Hu, B. C. Guo, S. Y. Pan, D Yan, M. C. Tang, and P. Wang: IEEE Trans. Circuits Syst. II Express Briefs **70** (2023) 91. https://doi.org/10.1109/TCSII.2022.3203718
24 K. Z. Hu, M. C. Tang, D. J. Li, Y. Wang, and M. Li: IEEE Trans. Antennas Propag. **68** (2020) 1134. https://doi.org/10.1109/TAP.2019.2938574


## About the Authors

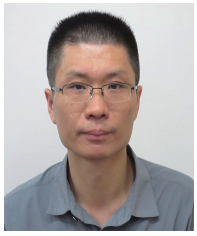

**Guo Tianwen** received his bachelor's degree from Chongqing University in China in 2002. In 2003 and 2017, he worked as an engineer at Longyan Cigarette Factory in China, and since 2018, he has been serving as a senior engineer at the factory. His research interests are in the Internet of Things, big data, and information technology. (gtw22338@fjtic.cn)

**Xu Yanggao** received his bachelor's degree from Fuzhou University in China in 1998. Since 1998, he has been working in the field of logistics automation and informatization at Longyan Tobacco Industry Co., Ltd. in China. His research interests are in industrial automation, the Internet of Things, and information technology. (xyg22210@fjtic.cn)

**Xie Yong** obtained his bachelor's degree from Jimei University in China in 2003. Since 2008, he has been working as an engineer at Longyan Tobacco Industry Co., Ltd. in China. His research interests are in automation, the Internet of Things, and information technology. (xy22345@fjtic.cn)

**Li Xiaogang** received his bachelor's degree from Fuzhou University in China in 1995. From 1995 to 2009, he worked as an engineer at Longyan Tobacco Industry Co., Ltd. in China, and since 2010, he has been a senior engineer at the factory. His research interests are in automatic control, logistics technology, and big data. (lxg22089@fjtic.cn)

**Lu Dahui** received his bachelor's degree from Tianjin Vocational and Technical Normal University in 2002. Since 2002, he has been working as an engineer at Longyan Tobacco Industry Co., Ltd. in China. His research interests include electrical automation, intelligent AGV, and Internet of Things technology. (ldh22334@fjtic.cn)

**Xing Haitao** was born in 1983 in Shandong, China. In 2010, he obtained his master's degree in communication and information engineering from Ningbo University. At present, his main research interests are in embedded systems, artificial intelligence, and Internet of Things, among others. (xht2005@jmu.edu.cn)

**Ma Zhonghua** was born in Gansu, China, in 1973. He received his Ph.D. degree in microelectronics from Lanzhou University in 2018. His present research interests include antenna techniques, RF circuit design, RFID systems, and Internet of Things. (mzhxm@jmu.edu.cn)